

**Structure–Activity Relationships Towards the Identification of High-Potency Selective  
Human Toll-Like Receptor-7 Agonist**

Deepender Kaushik,<sup>1</sup> Arshpreet Kaur,<sup>1</sup> Madhuri T. Patil,<sup>2</sup> Binita Sihag,<sup>1</sup> Sakshi Piplani,<sup>3,4</sup>  
Isaac Sakala,<sup>3,4</sup> Yoshikazu Honda-Okubo,<sup>3,4</sup> Saravanan Ramakrishnan,<sup>5</sup> Nikolai  
Petrovsky,<sup>3,4,\*</sup> Deepak B. Salunke<sup>1,6,\*</sup>

<sup>1</sup>Department of Chemistry and Centre of Advanced Studies in Chemistry, Panjab University,  
Chandigarh 160014, India

<sup>2</sup>Mehr Chand Mahajan DAV College for Women, Sector 36A, Chandigarh 160 036, India

<sup>3</sup>Vaxine Pty Ltd, 11 Walkley Avenue, Warradale, South Australia 5046, Australia

<sup>4</sup>College of Medicine and Public Health, Flinders University, Bedford Park, South Australia  
5042, Australia

<sup>5</sup>Immunology Section, Indian Veterinary Research Institute, Bareilly 243122, India

<sup>6</sup>National Interdisciplinary Centre of Vaccines, Immunotherapeutics and Antimicrobials  
(NICOVIA), Panjab University, Chandigarh 160 014, India

\*Corresponding authors: [salunke@pu.ac.in](mailto:salunke@pu.ac.in); [nikolai.petrovsky@flinders.edu.au](mailto:nikolai.petrovsky@flinders.edu.au)

## Abstract

Toll-like receptors (TLRs) act as the “sentinel” of the immune system to link innate immune responses with adaptive immunity. TLR7 agonists are highly immunostimulatory and can be exploited as powerful vaccine adjuvants. A structure-activity relationship study was conducted on the TLR7-active imidazoquinoline (IMDQ) scaffold, starting with 1-benzyl-2-butyl-1*H*-imidazo[4,5-*c*]quinolin-4-amine (BBIQ) as a lead structure. A systematic exploration of electron withdrawing as well as electron donating substituents at the *para*-position of benzyl group at *N*-1 position of IMDQ scaffold led to the identification of a highly active *para*-hydroxymethyl IMDQ analogue with an EC<sub>50</sub> value of 0.23 μM for human TLR7 with marginal activity for human TLR8, thereby indicating it as a TLR7-specific agonist that was 37-fold more potent than imiquimod. Its bio-steric *para*-aminomethyl analogue was a dual TLR7 and TLR8 agonist. Molecular modelling was performed which revealed the TLR8 activity of the IMDQ scaffold to be associated with the presence of amino functionality in the benzyl group. TLR7-biased activity was driven by the forming of multiple H-bonds with TLR7 which not formed when the IMDQ scaffold compounds were docked with TLR8. Finally, the role of the IMDQ scaffold agonists as vaccine adjuvants was tested with a Covid-19 vaccine in mice, which showed that TLR7 activity even in the absence of TLR8 activity was sufficient for potentiation of anti-spike protein antibody production, suggesting that TLR7 specific agonists may make suitable vaccine adjuvants.

**Key words:** Imidazoquinoline, TLR7, TLR8, vaccine, adjuvant, influenza, molecular modeling

## Introduction

Toll-like receptors (TLRs) are expressed on multiple cell types and serve as the first line of defense against invading pathogens. TLRs detect pathogen associated molecular patterns (PAMPs), characteristic molecular signatures on pathogens that allow the host to recognize the first signs of attack by an exogenous organism.<sup>1</sup> Among the 10 functional TLR's identified in humans, TLR-1, -2, -4, -5, -6 and -10 are expressed on the cellular plasma membrane while TLR-3, -7, -8 and -9 are expressed in the endosomal compartment.<sup>2-3</sup> Of the endosomal TLRs, TLR7 agonists stimulate lymphocyte subsets broadly but do not induce prominent pro-inflammatory cytokine responses.<sup>4-5</sup> On the other hand, TLR8 agonists induce inflammatory cytokines such as TNF- $\alpha$  and IL-12 as well as the chemotactic cytokine, MIP-1 $\alpha$ . TLR7-selective agonists have been found to be more effective than TLR8-selective agonists at inducing interferon (IFN)- $\alpha$  and IFN- $\gamma$ .<sup>6</sup> Several TLR7-selective agonists are in use as vaccine adjuvants and therapeutic drugs.<sup>7</sup> The TLR7 agonist, imiquimod (**1**, Figure 1), was approved by FDA in 1997 for the treatment of basal cell carcinoma and actinic keratosis.<sup>8</sup> SM-276001 (**2**) and GSK2245035 (**3**) from the 8-hydroxyadenine series are TLR7-selective agonists and are potent interferon inducers in both mice and monkeys.<sup>9-10</sup> GSK2245035 (**3**) was developed as a therapeutic agent against allergic rhinitis, asthma and respiratory allergies.<sup>7,11-12</sup> Vesatolimod (**4**) with 30-fold selectivity for hTLR7 over hTLR8 was examined in clinical trials to treat chronic hepatitis B (HBV) infection.<sup>13</sup> BBIQ (**5**), a TLR7 selective agonist has been explored as a vaccine adjuvant<sup>14</sup> and as an immunotherapeutic agent against *Plasmodium berghei* ANKA.<sup>15</sup> Most recently, a whole virion inactivated SARS-COV-2 vaccine (BBV152) adjuvanted with a TLR7 agonist adsorbed to alum adjuvant has been approved by FDA for use against COVID-19.<sup>16</sup>

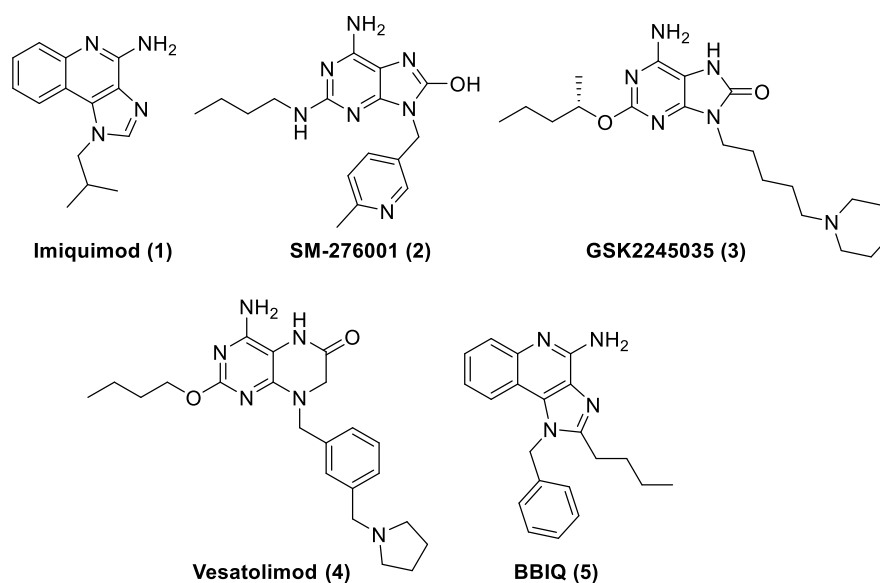


**Figure 1.** Small molecule TLR7 agonists in preclinical or clinical use.

Imidazoquinolines include potent TLR7 agonists.<sup>4</sup> The limited structural modifications on this series of compounds suggest that further structure activity relationship (SAR) studies on this scaffold may result in the identification of new potent TLR7 selective agonists.<sup>17</sup> With the aim to identify ligands with maximum selectivity of TLR7 over TLR8, we report here the synthesis and evaluation of a library of substituted 1*H*-imidazo[4,5-*c*]quinolines, amongst which we identified several highly potent TLR7 selective agonists with ~40 fold improved TLR7 activity over imiquimod.

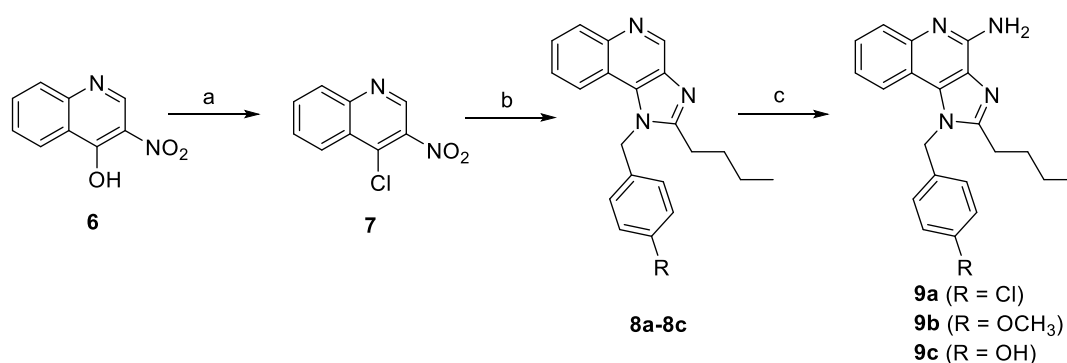
## Results and Discussion

In our vaccine adjuvant discovery program, we have systematically analyzed the SAR of all the known TLR7 and TLR8 agonist scaffolds.<sup>17</sup> During this investigation, 1-benzyl-2-butyl-1*H*-imidazo[4,5-*c*]quinolin-4-amine (**BBIQ**) was observed to be the most potent TLR7-specific imidazoquinoline (IMDQ). The substitution of an amino-methyl moiety at the para position on the benzyl group at *N*-1 in IMDQ is known to markedly improve both TLR7 and TLR8 activity. The limited SAR studies at this position<sup>18</sup> warrants further investigation. Therefore, to identify novel TLR7 selective IMDQs, a focused structural modification at the

*para*-position of benzyl group at *N*-1 with electron withdrawing as well as electron donating substituents was attempted.

Selection of a suitable synthetic route for the preparation of an IMDQ-based compound library was the first task. The TLR7 active IMDQs were previously synthesized *via* three different routes. David et al.<sup>19</sup> synthesized IMDQ scaffold starting from quinoline-2,4-diol or anthranilic acid, but low yield was a major issue. Fergusson et al.<sup>20</sup> synthesized an IMDQ library involving multicomponent condensation, Sandmeyer reaction as well as Suzuki–Miyaura coupling protocol. This approach involves several functionalized synthons and expensive reagents. We recently optimized a process for the synthesis of 1-benzyl-2-butyl-1*H*-imidazo[4,5-*c*]quinolin-4-amine (BBIQ) from a commercially available phthalimide and the complete process was optimized to improve the overall yield and cost effectiveness.<sup>14</sup> Following this synthetic route, 3-nitroquinolin-4-ol **6** was synthesized on a large scale and was further utilized for the preparation of a focused library.

**Scheme 1.** Synthesis of *para*-benzyl substituted IMDQs.



**Reagents and conditions:** (a) POCl<sub>3</sub>, reflux, 40 min, 92%; (b) (i) 4-chlorobenzylamine (for **8a**), 4-methoxybenzylamine (for **8b**), 4-hydroxybenzylamine (for **8c**), Et<sub>3</sub>N, CH<sub>2</sub>Cl<sub>2</sub>, reflux, 45 min, 93%; (ii) Pd/C, H<sub>2</sub>, EtOAc, Na<sub>2</sub>SO<sub>4</sub>, 4h, 95%; (iii) trimethylorthovalerate, toluene, reflux, 115 °C, 4h, 72%; (c) (i) 3-chloroperoxy benzoic acid, MeOH, CH<sub>2</sub>Cl<sub>2</sub>, reflux, 1h; 90% (ii) benzoyl isocyanate, CH<sub>2</sub>Cl<sub>2</sub>, reflux, 4 h; (iii) NaOCH<sub>3</sub>, anh. MeOH, 80 °C, 75% (2 steps)

Compound **6** on treatment with POCl<sub>3</sub> resulted in the formation of a chloro derivative **7**. The *ipso*-displacement of a chloro functionality with 4-chlorobenzylamine (for compound **8a**), 4-methoxybenzylamine (for compound **8b**) and 4-hydroxybenzylamine (for compound **8c**) was carried out as described earlier.<sup>14</sup> The nitro reduction was achieved using 1% palladium on activated charcoal (10% Pd basis) using rubber bladder filled with a hydrogen gas. The volatilities were removed by passing the reaction mixture through a bed of celite to obtain an intermediate amino derivative which without further purification was reacted with trimethylorthoalverate in toluene to furnish 1*H*-imidazo[4,5-*c*]quinoline derivatives (**8a-8c**). *N*-oxidation of quinoline nitrogen was carried out using 3-chloroperoxybenzoic acid in a solvent mixture of MeOH:dichloromethane for an hour, which on further reaction with benzoyl isocyanate followed by sodium methoxide resulted in the formation of desired 1*H*-imidazo[4,5-*c*]quinolin-4-amine derivatives (**9a-9b**) with C4 amino functionality. It is noteworthy to mention that the column chromatographic purification was required only twice in this whole synthetic process. On large scale reactions (5 gm), the final purification was also achieved using crystallization of the product in a mixture of 10% methanol in dichloromethane to obtain high purity samples (>99% purity, confirmed by HPLC).

The synthesized derivatives (**9a**, **9b** and **9c**) were screened for TLR7 and 8 activities using human TLR7 or TLR8-transfected HEK blue cell lines (Figure 2). The reporter cell assays confirmed that the parent BBIQ **5** as well as its chloro (**9a**) and methoxy (**9b**) analogs retained selective TLR7 agonist activities (EC<sub>50</sub> = 2.94 μM and EC<sub>50</sub> = 1.87 μM, respectively). The hydroxy derivative (**9c**) was found to be the most active TLR7 agonist in this series (EC<sub>50</sub> = 0.25 μM) with very little TLR8 agonistic activity (EC<sub>50</sub> = 30.02 μM).

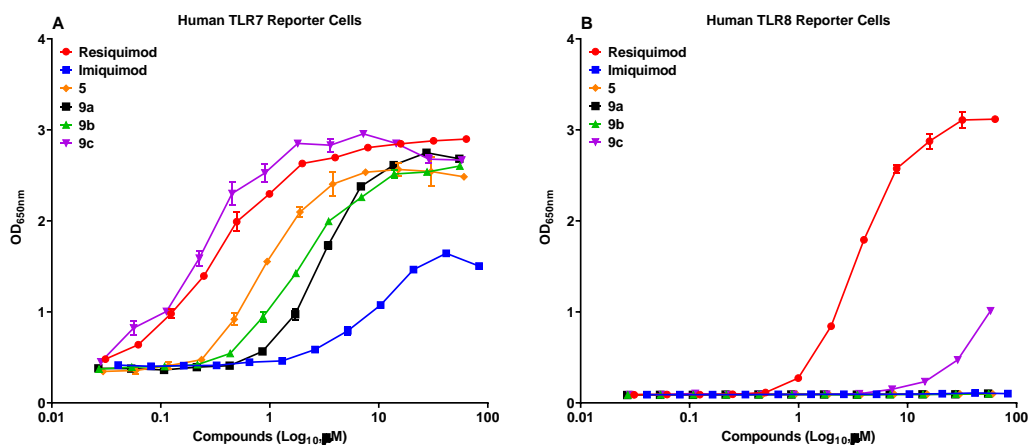
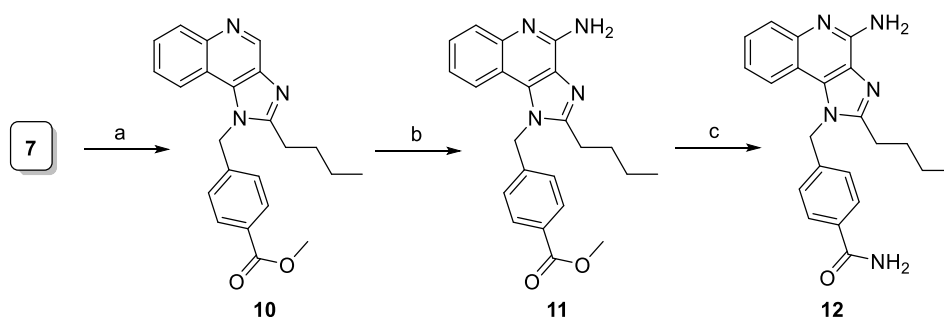


**Figure 2.** The relative potency of Resiquimod, Imiquimod, **5**, **9a**, **9b** and **9c** for human TLR7 and TLR8 was measured using HEK reporter cell lines transfected with human TLR7 (A) or TLR8 (B). Activation of NF- $\kappa$ B as a consequence of TLR7 or TLR8 activation by the ligand was quantified via secretion of alkaline phosphatase as a result of reporter activation. Shown is mean  $\pm$  standard error of the OD readings of duplicate samples.

We were also desirous to explore the role of terminal amide functionality at the *para*-position of the benzyl group. The synthesis of a desired benzamide derivative **12** was achieved from the ester analogue which was prepared following the same synthetic route (Scheme 1). Compound **11** on refluxing with 7% ammonia in methanol solution in a pressure vial yielded the desired benzamide **12**.

**Scheme 2.** Synthesis of amide analogues.

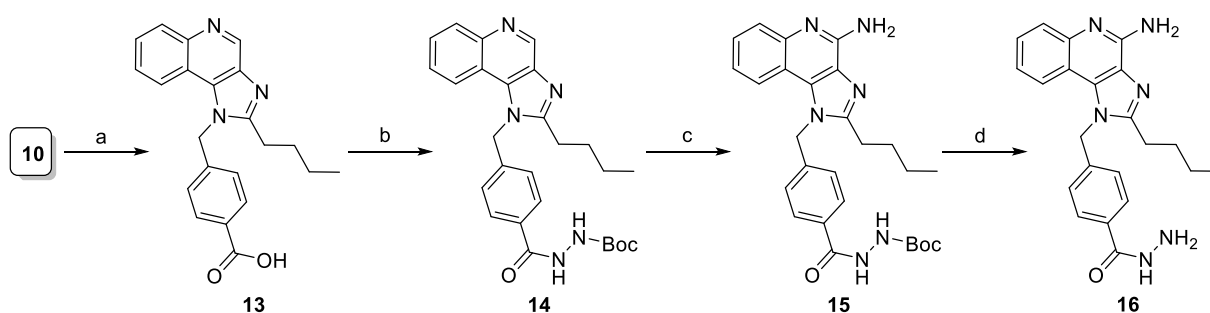


**Reagents and conditions:** (a) (i) methyl-4-(aminomethyl)benzoate, Et<sub>3</sub>N, CH<sub>2</sub>Cl<sub>2</sub>, reflux, 45 min; (ii) Pd/C, H<sub>2</sub>, EtOAc, Na<sub>2</sub>SO<sub>4</sub>, 4h; (iii) trimethylorthoalderate, toluene, reflux, 115 °C,

4h; (c) (i) 3-chloroperoxy benzoic acid, MeOH, CHCl<sub>3</sub>, CH<sub>2</sub>Cl<sub>2</sub>, reflux, 1h; (ii) benzoyl isocyanate, CH<sub>2</sub>Cl<sub>2</sub>, reflux, 4 h; NaOCH<sub>3</sub>, anh. MeOH, 80 °C, 1h; (d) 7% ammonia in MeOH solution, pressure vial, 110 °C, 10h.

The introduction of amine group in compound **12** (TLR7: EC<sub>50</sub> = 0.37 μM; TLR8: EC<sub>50</sub> = 17.48 μM) resulted in nearly 2-fold improvement in TLR7 activity as compared to BBIQ, with nearly 47-fold selectivity for TLR7 over TLR8. The compound **11** with ester functionality showed nearly 8-fold decline in the TLR7 agonistic activity as compared to its amide derivative **12**.

### Scheme 3. Synthesis of hydrazide analogues



**Reagents and conditions:** (a) 1N LiOH solution, MeOH, reflux, (b)  $\text{NH}_2\text{NHBoc}$ ,  $\text{Et}_3\text{N}$ , HOBt, EDCI, DMF; (c) (i) 3-chloroperoxy benzoic acid, MeOH,  $\text{CHCl}_3$ ,  $\text{CH}_2\text{Cl}_2$ , reflux, 1h; (ii) benzoyl isocyanate,  $\text{CH}_2\text{Cl}_2$ , reflux, 4 h;  $\text{NaOCH}_3$ , anh. MeOH, 80 °C, 1h; (d) HCl/dioxane, 2 h.

Based on these promising results, it was interesting to understand the effect of introduction of another nitrogen atom at the amide end of this molecule. Our first attempt for the direct substitution of hydrazine group on ester derivative (**11**) using *tert*-butylcarbazate in methanol at 110 °C failed. Therefore, ester hydrolysis followed by a coupling with *tert*-butylcarbazate in the presence of HOBt and EDCI on compound **10** was attempted which resulted in the formation of hydrazide **14** which on C4 amino installation via similar protocol as described in



Scheme 1 resulted in desired compound **16**. Both hydrazide (**16**) and its Boc protected derivative (**15**) were observed to be selective TLR7 agonists (Figure 3) but no improvement in the activity was observed. Being active, the hydrazide derivative can be utilized for the conjugation chemistry and might have better aqueous solubility.

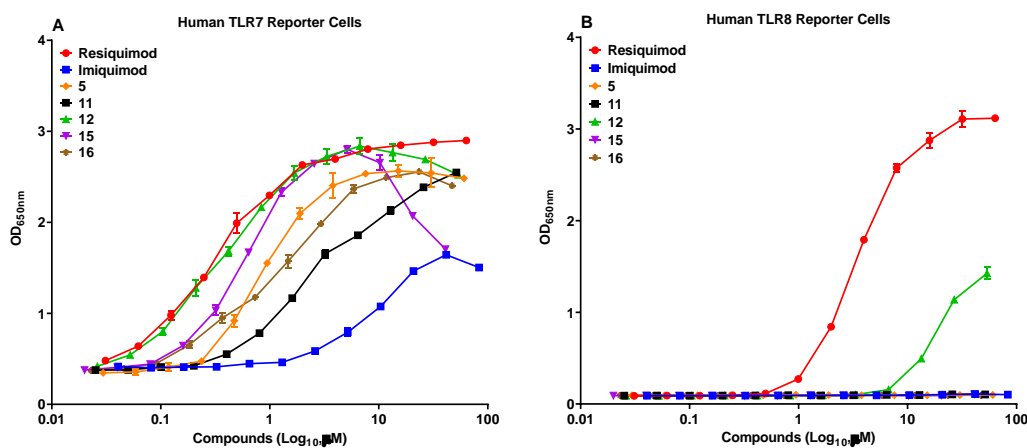
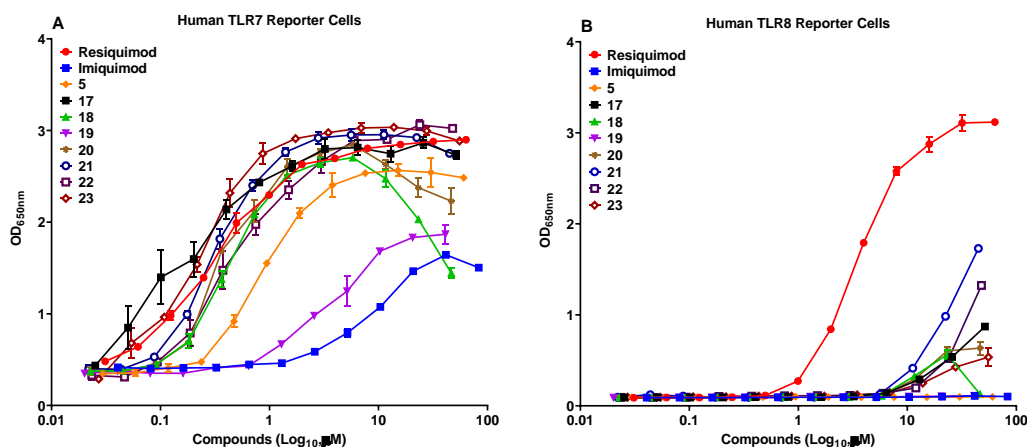


**Figure 3.** The relative potency of Resiquimod, Imiquimod, **5**, **11**, **12**, **15** and **16** for human TLR7 and TLR8 was measured using a reporter cell assay using HEK cell lines transfected with human TLR7 (A) or TLR8 (B) connected to a secreted alkaline phosphatase reporter.

To search for more potent TLR7 selective agonists, further derivatization at the amide nitrogen were performed. The desired *N*-alkyl derivatives, **17**, **18** and **19** were synthesized by the reaction of ester derivative **11** with different amines. Among the *N*-methyl (**17**), *N*-butyl (**18**) and *N*-octyl (**19**) derivatives, a linear relationship between alkyl chain length and TLR7 agonistic activity was observed. *N*-methyl (**17**, TLR7 EC<sub>50</sub> = 0.20 μM; TLR8 EC<sub>50</sub> = 20.96 μM) analogue was observed to be the most potent in the series and the agonistic activity was curtailed with the increase in the alkyl chain length (Figure 4). Compound **17** showed nearly 4-fold more TLR7 agonistic activity than BBIQ, with nearly 100-fold selectivity for TLR7 over TLR8 (Figure 3). But in case of *N*-isobutyl derivative (**20**) no improvement in the TLR7 agonistic activity was observed.

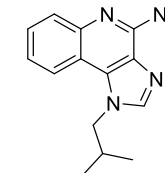
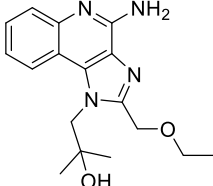
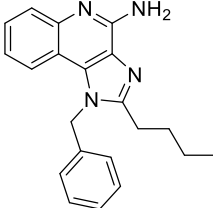
**Scheme 4.** Synthesis of amide analogues of compound **11**.

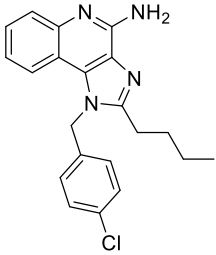
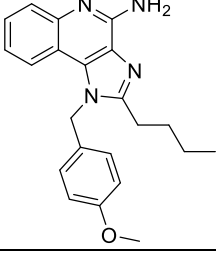
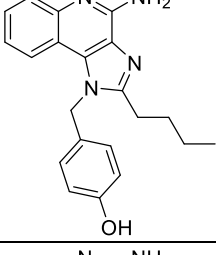
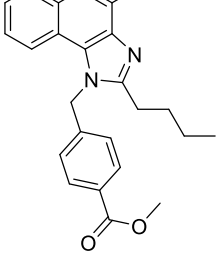
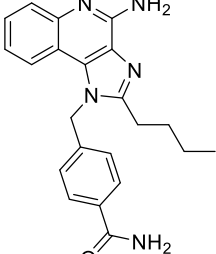
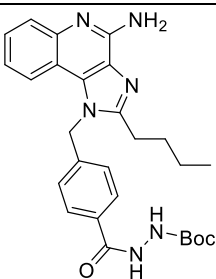


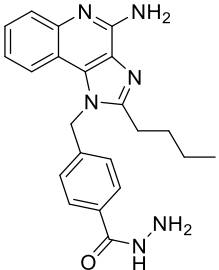
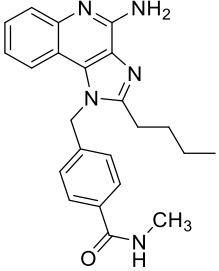
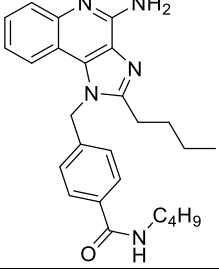
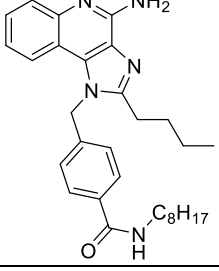
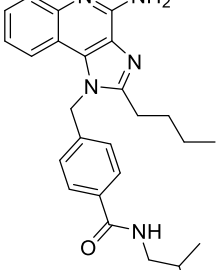
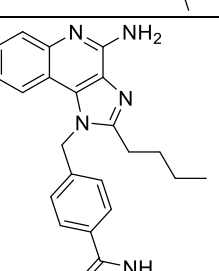


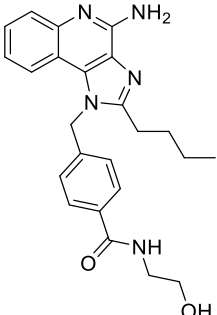
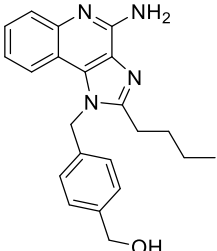
**Figure 4.** The relative potency of Resiquimod, Imiquimod, 5, 17, 18, 19, 20, 21, 22 and 23 for human TLR7 and TLR8 was measured using HEK reporter cell lines (InvivoGen) transfected with human TLR7 (A) or TLR8 (B).

**Table 1.** EC<sub>50</sub> value (μM) of compounds in human TLR7 and 8-specific reporter cell assay.

Compound Number	Structure	hTLR7 - Activity (μM)	hTLR8 - Activity (μM)
<b>Imiquimod</b>		8.38	13.15
<b>Resiquimod</b>		0.37	3.57
<b>5</b>		0.88	4.37

<b>9a</b>		2.94	7.18
<b>9b</b>		1.87	8.26
<b>9c</b>		0.25	30.02
<b>11</b>		2.81	4.33
<b>12</b>		0.37	17.48
<b>15</b>		0.58	17.92

<b>16</b>		1.10	1.21
<b>17</b>		0.20	20.96
<b>18</b>		0.43	32.27
<b>19</b>		3.39	6.23
<b>20</b>		0.40	13.04
<b>21</b>		0.33	19.87

22		0.57	26.42
23		0.23	17.21

### In silico structural analysis

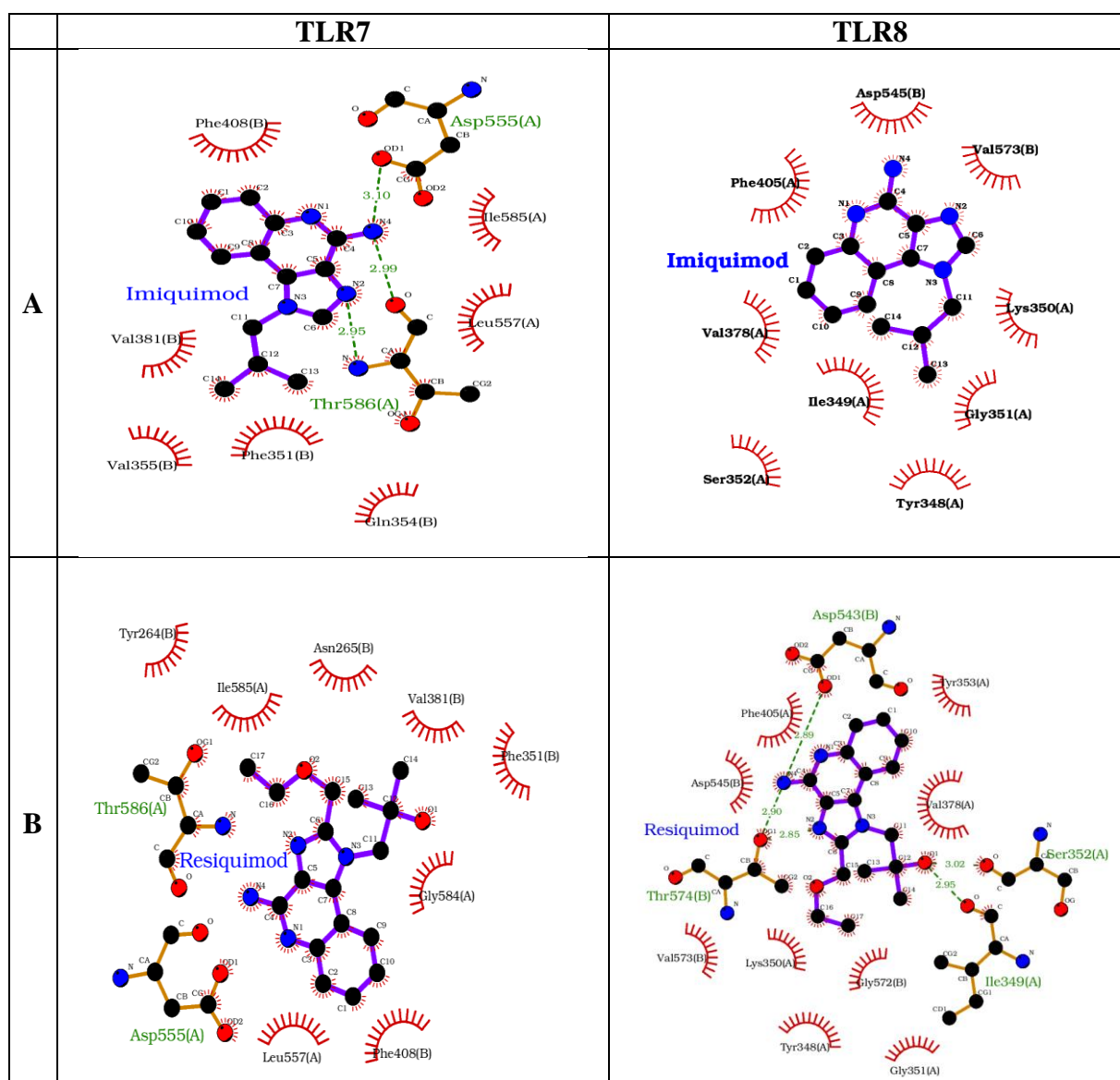
TLR7 and TLR8 are phylogenetically and functionally highly similar with a homologous horseshoe-shaped LRR region that contains the ligand binding site. Crystal structures have revealed that prior to ligand binding, the C-terminal domains are 53 Å apart, which prevents cytoplasmic domain association. When an agonist ligand binds to the TLR-7 or -8 homodimer, the two C-terminal domains come close to each other within 23 Å, and this expedites the dimerization of the TLR domains, which initiates the downstream signaling cascade resulting in immune cell activation. To better understand how the various BBIQ derivatives may bind to TLR7 and/or TLR8 and what interactions are responsible for achieving TLR7 specificity, we next performed docking studies with human TLR7 and TLR8 to characterize the interactions of these ligands with the binding pocket with the hope that this might then allow targeted design of new more potent agonists. For TLR7, the pocket formed by Phe408, Phe351 and Phe349 formed hydrophobic interactions with C-2 substituent of the compounds and this interaction was critical for TLR7 binding activity, although the hydrogen(H)-bonding interactions between the ligand and Thr586 and Asp555 were ultimately the driving force determining TLR7 activity. Conversely, for TLR8 activity, the

hydrogen bond interactions between the ligand and Asp543 and Gly351 in the TLR8 binding pocket were shown to be important. The hydrophobic cavity of TLR8 shared a very close border with another hydrophobic groove bounded by Phe346 and Tyr348. The N4 atoms of the imidazoquinoline scaffold was important in forming H-bonds with TLR7, thereby making the compounds more active towards TLR7.

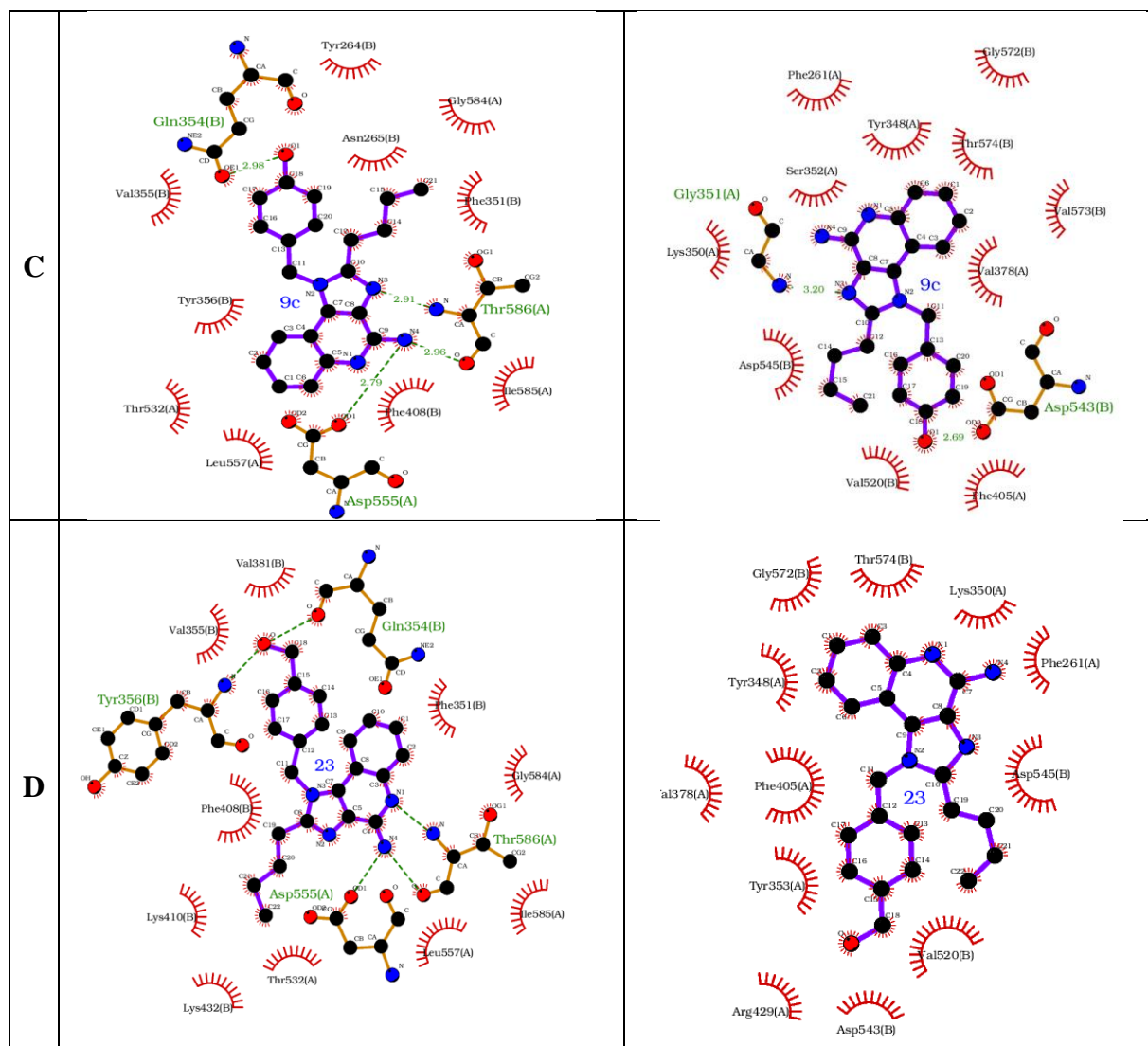
The docking analysis of Resiquimod, Imiquimod, BBIQ, and compounds **9a**, **9b**, **9c** and **23** with TLR7 revealed important interactions in which the N4 formed bifurcated H-bond with O of Asp555 and Thr586. Another N atom formed an H-bond with Thr586. The bicyclic ring system was involved in  $\pi$ - $\pi$  stacking arrangement with Phe405/Phe408 in both TLR7 and 8. In TLR8, Resiquimod forms H-bond with structurally conserved residues Asp543 and Thr574. Compound **9c** forms one H-bond with Gly351. Whereas, BBIQ and compound **9b** do not form the same H-bonds with TLR8 resulting in lack of activity. Imiquimod lacks the C-2 substitution and was found to specifically activate TLR7 and not TLR8. In particular, the compound **9c** was involved in a  $\pi$ - $\pi$  stacking arrangement with Phe408/Phe405 in TLR7/8 and the N4 and O1 atoms made a bifurcated hydrogen bond to the strictly conserved TLR7/8 Asp555/543 and to the backbone carbonyl of Thr586 as a H donor in TLR7 but not in TLR8 (Table 2). Compound **9c** was also engaged in H-bonding interaction with Gln354/Gly351 and this resulted in more extensive contacts and better target occupancies of TLR7 and TLR8, thereby conferring stronger binding affinity. Compound **9c** forms strong H-bonds with the key TLR7 residues, Asp555, Thr586 and Gln354. These three important residues favor the strong binding of **9c** to TLR7 compared to TLR8 where compound **9c** forms only one H-bond with Gly351 resulting in a loss of TLR8 activity. Interestingly, the hydroxyl group of compound **23** forms two H-bonds with Gln354 and Tyr356 and the N4 atom forms two bifurcated H-bonds with the two most important residues involved in TLR7 activity, Thr586

and Asp555. Additionally, Asp555 and Thr586 were able to stabilize compound **23** in the active site resulting in better target occupancy and stronger TLR7 binding affinity.

**Table 2.** Predicted docked conformations: Imiquimod (**A**), resiquimod (**B**), **9C** (**C**) and **23** (**D**) to the ligand-binding site of human TLR7, and Imiquimod (**E**), resiquimod (**F**), **9C** (**G**) and **23** (**H**) to the ligand-binding site of human TLR8, showing predicted hydrogen bonds in green.







The structural details showcasing the docked conformations of all the other analogs are included in the supporting information (Table S1). The O1 atom in the ester functionality of compound **11** led to the formation of a H-bond with the polar uncharged residue Asn265 and kept the H-bond interaction of Gln354 in TLR7. The N atom of Gly 351 forms H-bond with N4 atom of compound **11** with bond length of 3.30 Å, supporting both TLR7 and TLR8 activity. The amine nitrogen atoms (N1, N3 and N4) of compound **12** efficiently engages in a H-bond interaction with Thr586 and Asp555 in TLR7 and the amide group fits well into the deep hydrophobic pocket encompassed by Phe349, Phe466, and Thr586. Similarly, the amide group fits well in hydrophobic pocket of TLR8 where it formed two H-bonds with Ala518 and Gly351 (Table S1). The Boc derivative compound **15** formed a strong H-bond with polar

residue Gln354 in TLR7 and the purine scaffold formed an H-bond with TLR7 Thr586 and Asp555, whereas compound **15** lost these important interactions when docked on TLR8, confirming that the bulky Boc functionality in **15** hinders TLR8 agonistic activity. The oxygen atom of the hydrazide group in compound **16** resulted in the formation of three H-bonds with N atom of Thr586, ND2 of Asn265, and O atom of Gly584, respectively. Similarly, N4 in compound **17** made a bifurcated hydrogen bond to the conserved and important TLR7 Asp555 and Thr586 residues. The N3 and N4 residues formed important H-bonds with Asp555 in TLR7, and N1 and N4 formed H-bonds to Thr586. This suggests Asp555 and Thr586 are crucial residues to the activity of TLR7. N3 also forms a H-bond with N atom of Gly351 in TLR8 suggesting N4 is important for both TLR7 and TLR8 activity. In compound **18** n-butyl chain sits well in the TLR7 hydrophobic pocket and its O forms a strong H-bond with N of Thr586 whereas it forms no H-bonds with TLR8, explaining its lack of TLR8 activity. Compound **19** forms four H-bonds with TLR7. Atom N1 and N4 form H-bond with Tyr264 and Gln354. Furthermore, the introduction of different length chains to compounds **18** and **19** resulted in formation of different H-bonds compared to the other compounds and the addition of the chains also decreased TLR8 interaction due to steric clashes. The docking model showed that the increased chain length sterically clashed with atom CG1 of Val378 for compound **18** and Thr574 and Val520 with atom CG2. The amide group in compound **20** does not form any H-bond with the crucial residues of TLR8 whereas in TLR7 the N5 atom of amide group forms a strong H-Bond with NZ atom of Lys432. Compound **20** also forms  $\pi$ - $\pi$  stacking interaction and H-bonding with Tyr264 at the bottom of the active pocket enforcing the importance of the amide group for TLR7 binding only and correlating with a loss of TLR8 activity. For compound **21**, the hydroxyl group was engaged in H-bond interaction with N of Arg429 of TLR8 whereas the O formed the H-bond with the N of Lys432 and Lys410 explaining the TLR7 agonistic activity. The purine scaffold was

sandwiched between two hydrophobic residues Tyr264 and Ile585 forming  $\pi$ - $\pi$  stacking interactions. The O atom in compound **22** formed bifurcated H-bonds with O of Thr586 and N of polar uncharged residue Asn265. The benzamide alkyl chain was stabilized by hydrophobic interactions of Val381, Phe351, and Tyr264 in TLR7, whereas with TLR8, the N3 atom of compound **22** was also involved with ionic interactions with Gly351, which depicts that this compound may have both TLR7 and TLR8 activity, but more favorable TLR7 activity.

### **Immunization Data:**

Next, we sought to assess whether the TLR7 and TLR8 activity measured *in vitro* using reporter cell lines translated into vaccine adjuvant activity, *in vivo*. For these studies, all the compounds at 10 microgram doses were formulated with a recombinant spike protein Covid-19 vaccine and tested for their ability to enhance anti-spike protein antibody production in immunized mice when compared to immunization with spike protein alone or formulated with the know TLR7-specific agonist, imiquimod, or combined TLR7 and 8 agonists, resiquimod. Alum adjuvant was used as a positive control (Figure 5).

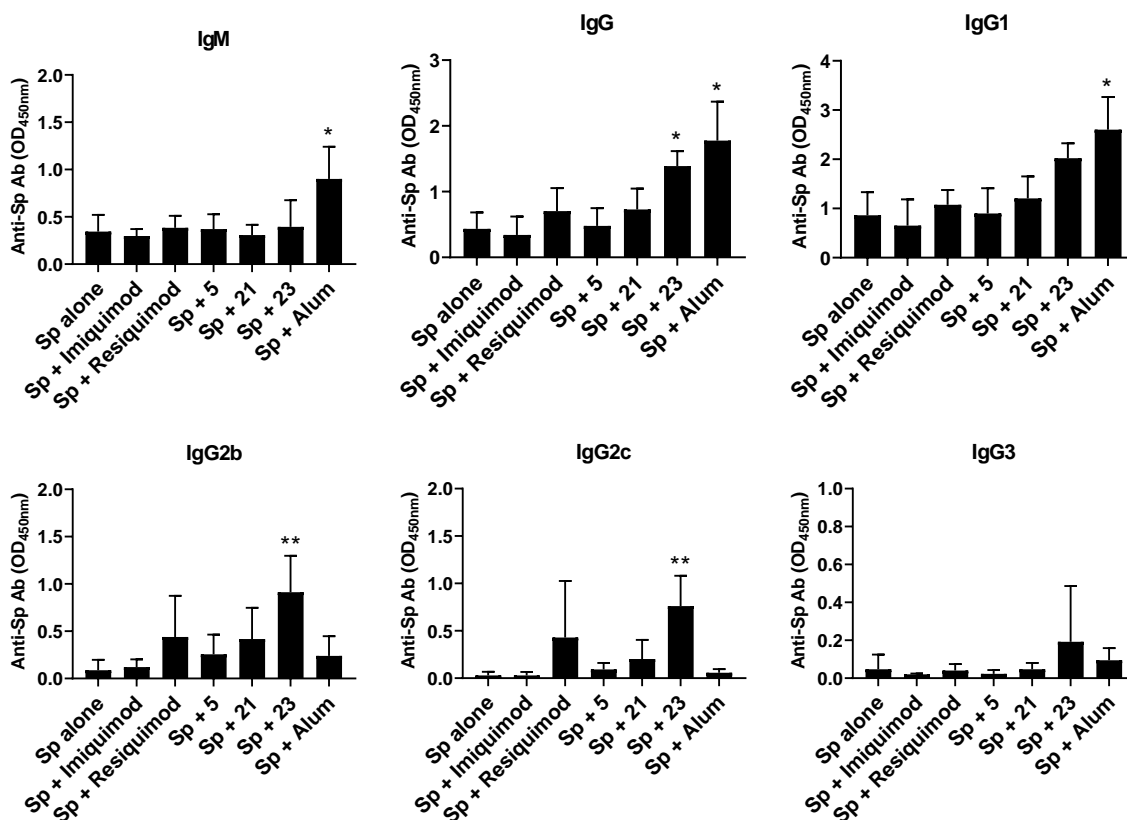


**Figure 5.** Anti-Sp antibodies responses in female C57BL/6 mice (n = 5 per group) after two intramuscular immunizations with Sp antigen with or without 10  $\mu$ g of TLR7/8 agonists or 50  $\mu$ g Alum. Blood samples were collected two weeks after the last immunization. Serum IgM and IgG antibodies were measured by ELISA (mean  $\pm$  SD). Statistical analysis was done using Kruskal–Wallis test. \*, p < 0.05 and \*\*, p < 0.01.

Spike protein alone induced only low amounts of antibody production with imiquimod not showing any adjuvant action. Similarly, resiquimod did not significantly increase antibody levels. Alum as expected imparted a strong T helper 2 (Th2) adjuvant effect, enhancing IgG1 but not IgG2b or IgG2c, production. The imidazoquinoline analogue **23** showed strong adjuvant activity on spike antibody levels which induced a strong Th1 response with increase in IgG2b and IgG2c, in addition to IgG1. Notably, the compound **23** was one of the most potent and TLR7 selective agonists with an activity for TLR7 of 0.23 micromolar, and no

measurable activity for TLR8. The Th1 bias imparted by TLR7 specific agonists may be secondary to their ability to enhance interferon production.

## Conclusions

A library of imidazoquinoline derivatives varying the electron withdrawing as well as electron donating groups at the *para*-position of benzyl substituent at N1 of the BBIQ scaffold was successfully synthesized to identify a novel pure TLR7 agonistic *para*-hydroxymethyl analogue **23**. Compound **23** was observed to be nearly 37-fold more potent selective TLR7 agonist than imiquimod and the TLR7 activity also correlated best with adjuvant activity *in vivo*, with a potent induction of a Th1 switch to IgG2b and IgG2c antibody production in immunized mice. Using an *in silico* molecular simulation and docking approach, it was possible to explain relative TLR7 specificity of the lead ligands, with the TLR7 specific compounds forming multiple H-Bonds with TLR7 but not with TLR8.

## 4. Experimental Section

### 4.1. Chemistry

Unless otherwise noted, all the reactions were conducted under an inert atmosphere (nitrogen or argon) using oven or flame-dried glassware. Solvents were dried following the standard procedures and for THF, it was freshly distilled before use. Unless otherwise mentioned, all reagents or catalysts were purchased from commercial sources and used without any further purification. Reactions were monitored by TLC, using Merck silica gel 60F 254 plates. Visualization of the TLC plates were performed either under UV light (254 nm) or by using 10% ethanolic phosphomolybdic acid (PMA) or 1% aqueous KMnO<sub>4</sub> or iodine. Flash column chromatography was performed using silica gel (230-400 mesh). <sup>1</sup>H and <sup>13</sup>C NMR spectra were recorded on Bruker Avance II (400 MHz) or Bruker Avance Neo (500 MHz) spectrometer after dissolving the samples in appropriate solvent. <sup>1</sup>H NMR chemicals shifts

are expressed in ppm ( $\delta$ ) relative to TMS or solvent peak. HRMS and Electron Spray Ionization (ESI) ( $m/z$ ) spectra were recorded on Agilent Technologies 6530 Accurate-Mass Q-TOF LC/MS. HPLC spectra was recorded on Agilent Technologies 1260 infinity.

**4.1.1. 4-chloro-3-nitroquinoline (7):** A suspension of compound **6** (3.0 g, 15 mmol) in  $\text{POCl}_3$  (9.0 mL, 96 mmol) was heated to reflux for an hour till a clear solution was obtained. The reaction mixture was cooled to 0 °C in ice bath and the cold solution was added drop wise on the crushed ice in a beaker to obtain a precipitate. The solid obtained was extracted in ethyl acetate (200 mL x 3) and the organic layer was washed with water and sodium hydrogen carbonate solution and dried over  $\text{Na}_2\text{SO}_4$ . The evaporation of the extract resulted in the formation of desired compound **28** which was used as it is for the next reaction (3.0 g, 92%).

**4.1.2. 2-butyl-1-(4-chlorobenzyl)-1*H*-imidazo[4,5-*c*]quinoline (8a):** To a solution of compound **7** (1.00 g, 4.8 mmol) in anhydrous dichloromethane (20 mL) were added triethylamine (1.01 mL, 7.2 mmol) and 4-chlorobenzylamine (760  $\mu\text{L}$ , 6.25 mmol). The reaction mixture was refluxed at 45 °C for 45 min. The solvent was then evaporated under vacuum, and water was added to the residue to obtain the precipitate. The precipitate was filtered, washed several times with water, and dried to obtain intermediate *N*-(4-chlorobenzyl)-3-nitroquinolin-4-amine as yellow solid (1.4 g, 93%). To a solution of *N*-(4-chlorobenzyl)-3-nitroquinolin-4-amine (500 mg, 1.59 mmol) in EtOAc (20 mL) were added palladium on activated charcoal (10% Pd basis, 5 mg, 1% w/w) and  $\text{Na}_2\text{SO}_4$  (100 mg). The reaction mixture was stirred under hydrogen atmosphere for 4 h. The reaction mixture was then filtered through celite, bed and the filtrate was evaporated under reduced pressure to obtain *N*<sup>4</sup>-(4-chlorobenzyl)quinoline-3,4-diamine as thick solid and used as it is for further reaction without any purification (430 mg, 95%). To a solution of *N*<sup>4</sup>-(4-chlorobenzyl)quinoline-3,4-diamine (400 mg, 1.40 mmol) in anhydrous toluene (10 mL) was

added trimethylorthovalerate (729  $\mu\text{L}$ , 4.23 mmol) and the reaction mixture was refluxed at 110  $^{\circ}\text{C}$  for 4 h. The solvent was evaporated and the crude product obtained was purified by flash column chromatography (3% MeOH/DCM) to yield desired product **8a** as off-white solid (350 mg, 72%).  $^1\text{H}$  NMR (400 MHz,  $\text{CDCl}_3$ )  $\delta$  9.35 (s, 1H), 8.25 (d,  $J = 8.3$  Hz, 1H), 7.85 (d,  $J = 8.3$  Hz, 1H), 7.61 (t,  $J = 7.4$  Hz, 1H), 7.43 (t,  $J = 7.4$  Hz, 1H), 7.30 (d,  $J = 8.3$  Hz, 2H), 6.98 (d,  $J = 8.2$  Hz, 2H), 5.75 (s, 2H), 2.97 – 2.86 (m, 2H), 1.95 – 1.82 (m, 2H), 1.54 – 1.40 (m, 2H), 0.95 (t,  $J = 7.3$  Hz, 3H). HRMS  $m/z$ : calculated for  $\text{C}_{21}\text{H}_{21}\text{ClN}_3^+$  [ $\text{M} + \text{H}$ ] $^+$  350.1419, found 350.1419.

**4.1.2. 2-butyl-1-(4-methoxybenzyl)-1H-imidazo[4,5-c]quinoline (8b):**  $^1\text{H}$  NMR (400 MHz,  $\text{CDCl}_3$ )  $\delta$  9.35 (s, 1H), 8.25 (dd,  $J = 8.3, 0.6$  Hz, 1H), 7.96 (dd,  $J = 8.4, 0.8$  Hz, 1H), 7.65 – 7.58 (m, 1H), 7.48 – 7.40 (m, 1H), 6.97 (d,  $J = 8.7$  Hz, 2H), 6.88 – 6.81 (m, 2H), 5.75 (s, 2H), 3.76 (s, 3H), 2.94 (t, 2H), 1.93 – 1.83 (m, 2H), 1.52 – 1.41 (m, 2H), 0.95 (t,  $J = 7.4$  Hz, 3H).  $^{13}\text{C}$  NMR (126 MHz,  $\text{CDCl}_3$ )  $\delta$  159.5, 156.0, 145.1, 144.8, 136.7, 134.3, 130.9, 127.1, 126.9, 126.9, 126.5, 120.1, 117.8, 114.9, 55.4, 48.6, 29.8, 27.3, 22.7, 13.9. MS  $m/z$ : calculated for  $\text{C}_{22}\text{H}_{24}\text{N}_3\text{O}^+$  [ $\text{M} + \text{H}$ ] $^+$  346.20, found 346.19.

**4.1.3. 4-((2-butyl-1H-imidazo[4,5-c]quinolin-1-yl)methyl)phenol (8c):**  $^1\text{H}$  NMR (500 MHz,  $\text{DMSO}-d_6$ )  $\delta$  9.41 (s, 1H), 9.20 (s, 1H), 8.15 (dd,  $J = 8.4, 0.7$  Hz, 1H), 8.12 (dd,  $J = 8.4, 1.0$  Hz, 1H), 7.65 – 7.59 (m, 1H), 7.54 – 7.48 (m, 1H), 6.86 (d,  $J = 8.6$  Hz, 2H), 6.72 – 6.67 (m, 2H), 5.83 (s, 2H), 2.96 (t, 2H), 1.82 – 1.74 (m, 2H), 1.45 – 1.36 (m, 2H), 0.89 (t,  $J = 7.4$  Hz, 3H).  $^{13}\text{C}$  NMR (126 MHz,  $\text{DMSO}-d_6$ )  $\delta$  156.7, 156.0, 144.2, 144.0, 136.2, 133.4, 130.1, 126.8, 126.5, 126.3, 126.1, 120.7, 117.3, 115.7, 47.7, 29.0, 26.2, 21.8, 13.7. MS  $m/z$ : calculated for  $\text{C}_{21}\text{H}_{22}\text{N}_3\text{O}^+$  [ $\text{M} + \text{H}$ ] $^+$  332.18, found 332.1.

**4.1.4. 2-butyl-1-(4-chlorobenzyl)-1H-imidazo[4,5-c]quinolin-4-amine (9a):** To a solution of compound **8a** (320 mg, 0.92 mmol) in a solvent mixture of MeOH:dichloromethane (0.1:1, 20 mL) was added 3-chloroperoxybenzoic acid (395 mg, 2.29 mmol) and the solution was

refluxed at 45-50 °C for 1h. The solvent was evaporated under reduced pressure and the residue was purified using flash column chromatography (6% MeOH/dichloromethane) to obtain intermediate 2-butyl-1-(4-chlorobenzyl)-1*H*-imidazo[4,5-*c*]quinoline-5-oxide as off-white solid (301 mg, 90%). To the solution of *N*-oxide (301 mg, 0.82 mmol) in anhydrous dichloromethane (10 mL), benzoyl isocyanate (242 mg, 1.64 mmol) was added and the resulting mixture was heated to reflux for 30 min. The solvent was removed under vacuum, and the residue was dissolved in anhydrous MeOH, followed by the addition of sodium methoxide (444 mg, 8.22 mmol). The reaction mixture was heated at 80 °C for 1h. The solvent was removed under vacuum, and the residue was purified using flash column chromatography (5% MeOH/dichloromethane) to obtain the desired product **9a** as white solid (225 mg, 75%). <sup>1</sup>H NMR (500 MHz, DMSO-*d*<sub>6</sub>) δ 7.76 (d, *J* = 8.0 Hz, 1H), 7.58 (d, *J* = 8.0 Hz, 1H), 7.39 (d, *J* = 8.5 Hz, 2H), 7.37 – 7.31 (m, 1H), 7.09 – 7.01 (m, 3H), 6.65 (s, 2H), 5.87 (s, 2H), 2.90 (t, 2H), 1.74 – 1.65 (m, 2H), 1.41 – 1.32 (m, 2H), 0.86 (t, *J* = 7.4 Hz, 3H). <sup>13</sup>C NMR (126 MHz, DMSO-*d*<sub>6</sub>) δ 153.9, 151.4, 151.4, 135.7, 133.0, 132.0, 128.9, 127.5, 126.7, 126.3, 121.3, 120.1, 114.2, 47.5, 29.6, 26.2, 21.8, 13.7. HRMS *m/z*: calculated for C<sub>21</sub>H<sub>22</sub>ClN<sub>4</sub><sup>+</sup> [*M* + *H*]<sup>+</sup> 365.1528, found 365.1526.

**4.1.5. 2-butyl-1-(4-methoxybenzyl)-1*H*-imidazo[4,5-*c*]quinolin-4-amine (9b):** <sup>1</sup>H NMR (400 MHz, CDCl<sub>3</sub>) δ 7.81 (dd, *J* = 8.3, 0.6 Hz, 1H), 7.74 (dd, *J* = 8.3, 0.8 Hz, 1H), 7.48 – 7.41 (m, 1H), 7.18 – 7.11 (m, 1H), 6.97 (d, *J* = 8.7 Hz, 2H), 6.88 – 6.80 (m, 2H), 5.95 (s, 2H), 5.66 (s, 2H), 3.76 (s, 3H), 2.88 (t, *J* = 7.84, 2H), 1.85 – 1.74 (m, 2H), 1.51 – 1.37 (m, 2H), 0.93 (t, *J* = 7.4 Hz, 3H). <sup>13</sup>C NMR (101 MHz, CDCl<sub>3</sub>) δ 159.5, 154.4, 151.1, 143.5, 134.3, 127.5, 127.2, 126.9, 126.6, 126.2, 122.7, 120.0, 115.0, 114.8, 55.4, 48.5, 30.1, 27.3, 22.7, 13.9. HRMS *m/z*: calculated for C<sub>22</sub>H<sub>25</sub>N<sub>4</sub>O<sup>+</sup> [*M* + *H*]<sup>+</sup> 361.2023, found 361.2028.

**4.1.6. 4-((4-amino-2-butyl-1*H*-imidazo[4,5-*c*]quinolin-1-yl)methyl)phenol (9c):** <sup>1</sup>H NMR (500 MHz, DMSO-*d*<sub>6</sub>) δ 9.44 (s, 1H), 7.85 (d, *J* = 8.2 Hz, 1H), 7.61 (d, *J* = 8.3 Hz, 1H), 7.38



(t,  $J = 7.6$  Hz, 1H), 7.11 (d,  $J = 7.5$  Hz, 1H), 6.90 (s, 2H), 6.85 (d,  $J = 8.2$  Hz, 2H), 6.70 (d,  $J = 8.2$  Hz, 2H), 5.73 (s, 2H), 2.90 (t,  $J = 7.7$  Hz, 2H), 1.74 – 1.65 (m, 2H), 1.42 – 1.32 (m, 2H), 0.86 (t,  $J = 7.3$  Hz, 3H).  $^{13}\text{C}$  NMR (126 MHz, DMSO- $d_6$ )  $\delta$  156.7, 154.1, 151.2, 133.3, 126.8, 126.4, 126.1, 124.9, 121.5, 120.5, 115.7, 114.3, 47.7, 29.5, 26.3, 21.8, 13.7. HRMS  $m/z$ : calculated for  $\text{C}_{21}\text{H}_{23}\text{N}_4\text{O}^+$   $[\text{M} + \text{H}]^+$  347.18664, found 347.18695.

#### 4.1.7. Methyl-4-((2-butyl-1H-imidazo[4,5-c]quinolin-1-yl)methyl)benzoate (10):

Compound **10** was synthesized similarly as described for compound **8a**.  $^1\text{H}$  NMR (500 MHz,  $\text{CDCl}_3$ )  $\delta$  9.37 (s, 1H), 8.27 (d,  $J = 8.4$  Hz, 1H), 8.01 (d,  $J = 8.3$  Hz, 2H), 7.83 (d,  $J = 8.4$  Hz, 1H), 7.60 (t,  $J = 7.7$  Hz, 1H), 7.41 (t,  $J = 7.7$  Hz, 1H), 7.12 (d,  $J = 8.2$  Hz, 2H), 5.85 (s, 2H), 3.89 (s, 3H), 2.96 – 2.90 (m, 2H), 1.92 – 1.85 (m, 2H), 1.51 – 1.42 (m, 2H), 0.94 (t,  $J = 7.4$  Hz, 3H).  $^{13}\text{C}$  NMR (126 MHz,  $\text{CDCl}_3$ )  $\delta$  166.5, 155.8, 145.0, 144.8, 140.3, 136.6, 134.1, 131.0, 130.8, 130.4, 127.0, 126.6, 125.6, 119.7, 117.5, 52.4, 48.9, 29.7, 27.3, 22.6, 13.9. HRMS  $m/z$ : calculated for  $\text{C}_{23}\text{H}_{24}\text{N}_3\text{O}_2^+$   $[\text{M} + \text{H}]^+$  374.1863, found 374.1848.

#### 4.1.8. Methyl-4-((4-amino-2-butyl-1H-imidazo[4,5-c]quinolin-1-yl)methyl)benzoate (11):

Compound **11** was synthesized similarly as described for compound **9a**.  $^1\text{H}$  NMR (500 MHz, DMSO- $d_6$ )  $\delta$  9.02 (s, 2H), 7.94 – 7.89 (m, 2H), 7.88 (dd,  $J = 8.3, 0.7$  Hz, 1H), 7.78 (dd,  $J = 8.4, 0.7$  Hz, 1H), 7.62 – 7.57 (m, 1H), 7.34 – 7.30 (m, 1H), 7.22 (d,  $J = 8.5$  Hz, 2H), 6.06 (s, 2H), 3.80 (s, 3H), 3.00 – 2.93 (m, 2H), 1.75 – 1.66 (m, 2H), 1.42 – 1.31 (m, 2H), 0.84 (t,  $J = 7.4$  Hz, 3H).  $^{13}\text{C}$  NMR (126 MHz, DMSO- $d_6$ )  $\delta$  165.9, 157.1, 149.1, 141.2, 135.5, 134.1, 130.0, 129.6, 129.3, 126.2, 125.0, 124.8, 121.6, 118.7, 116.4, 114.1, 112.5, 52.2, 48.5, 29.4, 26.4, 21.8, 13.6. HRMS  $m/z$ : calculated for  $\text{C}_{23}\text{H}_{25}\text{N}_4\text{O}_2^+$   $[\text{M} + \text{H}]^+$  389.1972, found 389.1971.

#### 4.1.9. 4-((4-amino-2-butyl-1H-imidazo[4,5-c]quinolin-1-yl)methyl)benzamide (12):

To the compound **11** (50 mg, 0.12 mmol) in pressure vials was added 7% ammonia in MeOH solution (5 mL) and refluxed at 110 °C for 10 h. The solvent was removed under vacuum, and

the residue was purified using flash column chromatography (10% MeOH/dichloromethane) to obtain the desired product **12** as solid (25 mg, 47%). <sup>1</sup>H NMR (500 MHz, DMSO-*d*<sub>6</sub>) δ 7.90 (s, 1H), 7.80 (d, *J* = 8.4 Hz, 2H), 7.74 (dd, *J* = 8.3, 1.0 Hz, 1H), 7.57 (dd, *J* = 8.3, 1.0 Hz, 1H), 7.35-7.29 (m, 2H), 7.09 (d, *J* = 8.4 Hz, 2H), 7.04-6.99 (m, 1H), 6.54 (s, 2H), 5.92 (s, 2H), 2.91 (t, 2H), 1.74-1.67 (m, 2H), 1.42-1.33 (m, 2H), 0.86 (t, *J* = 7.4 Hz, 3H). <sup>13</sup>C NMR (126 MHz, DMSO-*d*<sub>6</sub>) δ 167.4, 153.6, 151.7, 144.8, 139.9, 133.5, 132.8, 128.1, 126.5, 126.3, 126.1, 125.4, 120.9, 120.0, 114.5, 47.9, 29.6, 26.2, 21.8, 13.6. HRMS *m/z*: calculated for C<sub>22</sub>H<sub>24</sub>N<sub>5</sub>O<sup>+</sup> [M + H]<sup>+</sup> 374.1975, found 374.1972

**4.1.10. 4-((2-butyl-1*H*-imidazo[4,5-*c*]quinolin-1-yl)methyl)benzoic acid (13):** To a solution of compound **10** (270 mg, 0.72 mmol) in 20 mL MeOH was added 1N LiOH solution to adjust the pH 10 and refluxed for 10 h. The solvent was removed under vacuum, and neutralized the residue by adding 1M HCl solution drop-wise to precipitate out the compound. The product obtained was filtered, washed several times with cold water and dried in oven at 60 °C to obtain the desired product **13** (240 mg) as off-white solid, which was used as it is for the next reaction.

**4.1.11. *tert*-butyl-2-(4-((2-butyl-1*H*-imidazo[4,5-*c*]quinolin-1-yl)methyl)benzoyl)hydrazine-1-carboxylate (14):** To a solution of compound **13** (240 mg, 0.66 mmol) in DMF (10 mL) was added triethylamine (448 μl, 3.20 mmol) and HoBt (173 mg, 1.28 mmol), and stirred for 25 min. in an ice bath to maintained the temperature 0-5 °C. After 25 min. added EDCI (369 mg, 1.92 mmol) and remove the ice bath to bring the reaction mixture at room temperature. The reaction mixture was stirred at room temperature for 5h. Added the reaction mixture in ice-water bath and extract the compound in EtOAc using sodium bicarbonate. The solvent was removed under vacuum and the residue was purified using flash column chromatography (5% MeOH/dichloromethane) to obtain the desired product **14** as off-white solid (270 mg, 85%). <sup>1</sup>H NMR (500 MHz, DMSO-*d*<sub>6</sub>) δ 10.13 (d, *J* =

0.9 Hz, 1H), 9.22 (s, 1H), 8.88 (s, 1H), 8.12 (d,  $J = 8.4$  Hz, 1H), 8.05 (d,  $J = 8.3$  Hz, 1H), 7.79 (d,  $J = 8.0$  Hz, 2H), 7.64 – 7.58 (m, 1H), 7.50 – 7.45 (m, 1H), 7.13 (d,  $J = 8.4$  Hz, 2H), 6.05 (s, 2H), 2.98 (t,  $J = 7.6$  Hz, 2H), 1.81 – 1.73 (m, 2H), 1.45 – 1.27 (m, 11H), 0.88 (t,  $J = 7.4$  Hz, 3H).  $^{13}\text{C}$  NMR (126 MHz, DMSO- $d_6$ )  $\delta$  165.5, 156.0, 155.3, 144.2, 143.9, 140.1, 136.2, 133.3, 131.7, 130.1, 128.0, 126.5, 126.1, 125.5, 120.4, 117.1, 79.1, 47.9, 28.9, 28.0, 26.1, 21.6, 13.6. HRMS  $m/z$ : calculated for  $\text{C}_{27}\text{H}_{32}\text{N}_5\text{O}_3^+$   $[\text{M} + \text{H}]^+$  474.2500, found 474.2502.

**4.1.12. *tert*-butyl-2-(4-((4-amino-2-butyl-1*H*-imidazo[4,5-*c*]quinolin-1-yl)methyl)benzoyl)hydrazine-1-carboxylate (15):** Compound **15** was synthesized similarly as described for compound **9a**.  $^1\text{H}$  NMR (500 MHz, DMSO- $d_6$ )  $\delta$  10.13 (s, 1H), 8.87 (s, 1H), 7.79 (d,  $J = 8.0$  Hz, 2H), 7.72 (d,  $J = 7.8$  Hz, 1H), 7.57 (dd,  $J = 8.4, 1.1$  Hz, 1H), 7.35 – 7.29 (m, 1H), 7.13 (d,  $J = 8.4$  Hz, 2H), 7.04 – 6.99 (m, 1H), 6.55 (s, 2H), 5.94 (s, 2H), 2.94 – 2.89 (m, 2H), 1.74 – 1.65 (m, 2H), 1.44 – 1.29 (m, 11H), 0.86 (t,  $J = 7.4$  Hz, 3H).  $^{13}\text{C}$  NMR (126 MHz, DMSO- $d_6$ )  $\delta$  153.6, 151.7, 144.8, 140.6, 132.8, 128.0, 126.5, 126.4, 126.1, 125.6, 120.9, 120.0, 114.8, 79.2, 63.1, 47.9, 29.6, 28.1, 26.2, 21.8, 13.7. HRMS  $m/z$ : calculated for  $\text{C}_{27}\text{H}_{33}\text{N}_6\text{O}_3^+$   $[\text{M} + \text{H}]^+$  489.2609, found 489.2608

**4.1.13. 4-((4-amino-2-butyl-1*H*-imidazo[4,5-*c*]quinolin-1-yl)methyl)benzohydrazide (16):** To a solution of compound **15** (50 mg, 0.10 mmol) in 10 mL of HCl/dioxane was stirred at room temperature for 10h. The solvent was removed under vacuum to obtain the desired compound **16** (35 mg, 90%).  $^1\text{H}$  NMR (500 MHz, DMSO- $d_6$ )  $\delta$  13.99 (s, 1H), 11.70 (s, 1H), 7.92 – 7.80 (m, 3H), 7.73 (d,  $J = 8.0$  Hz, 1H), 7.56 (t,  $J = 7.4$  Hz, 1H), 7.28 (t,  $J = 7.4$  Hz, 1H), 7.18 (d,  $J = 7.9$  Hz, 2H), 6.01 (s, 2H), 2.91 (t,  $J = 7.5$  Hz, 2H), 1.72 – 1.58 (m, 2H), 1.38 – 1.24 (m, 2H), 0.79 (t,  $J = 7.2$  Hz, 3H).  $^{13}\text{C}$  NMR (126 MHz, DMSO- $d_6$ )  $\delta$  165.3, 156.9, 148.9, 140.5, 135.3, 133.6, 129.8, 129.5, 128.5, 125.9, 124.7, 124.7, 121.4, 118.4, 112.2,

48.2, 29.2, 26.1, 21.6, 13.6. MS m/z: calculated for C<sub>22</sub>H<sub>25</sub>N<sub>6</sub>O<sup>+</sup> [M + H]<sup>+</sup> 389.21, found 389.20.

**4.1.14. 4-((4-amino-2-butyl-1H-imidazo[4,5-c]quinolin-1-yl)methyl)-N-methylbenzamide**

**(17):** Compound **11** (50 mg, 0.13 mmol) was dissolved in 5 mL methylamine in methanol solution and reflux for 10h in pressure vial at 110 °C. The solvent was removed under vacuum and the residue was purified using flash column chromatography (10% MeOH/dichloromethane) to obtain the desired product **17** (45 mg, 90%) as off-white solid. <sup>1</sup>H NMR (500 MHz, CDCl<sub>3</sub>) δ 7.74 (d, *J* = 8.6 Hz, 1H), 7.71 (d, *J* = 8.3 Hz, 2H), 7.56 (d, *J* = 8.0 Hz, 1H), 7.37 (t, *J* = 7.6 Hz, 1H), 7.07 (t, *J* = 7.6 Hz, 1H), 7.02 (d, *J* = 8.2 Hz, 2H), 6.58 (d, *J* = 4.7 Hz, 1H), 6.24 (s, 2H), 5.71 (s, 2H), 2.92 (d, *J* = 4.8 Hz, 3H), 2.86 – 2.78 (m, 2H), 1.78 – 1.70 (m, 2H), 1.45 – 1.35 (m, 2H), 0.89 (t, *J* = 7.4 Hz, 3H). <sup>13</sup>C NMR (126 MHz, CDCl<sub>3</sub>) δ 167.5, 154.6, 150.9, 138.6, 134.8, 134.3, 128.1, 127.8, 126.5, 125.8, 125.6, 123.0, 119.8, 114.6, 48.8, 30.0, 27.3, 27.0, 22.6, 13.9 HRMS m/z: calculated for C<sub>23</sub>H<sub>26</sub>N<sub>5</sub>O<sup>+</sup> [M + H]<sup>+</sup> 388.2132, found 388.2125.

**4.1.15. 4-((4-amino-2-butyl-1H-imidazo[4,5-c]quinolin-1-yl)methyl)-N-butylbenzamide**

**(18):** To a solution of compound **11** (50 mg, 0.13 mmol) in 5 mL methanol was added n-butylamine (63 μl, 0.65 mmol) and reflux at 110 °C in pressure vial for 10h. The solvent was removed under vacuum and the residue was purified using flash column chromatography (8% MeOH/dichloromethane) to obtain the desired product **18** (43 mg, 81%) as off-white solid. <sup>1</sup>H NMR (500 MHz, CDCl<sub>3</sub>) δ 7.77 (d, *J* = 8.1 Hz, 1H), 7.71 (d, *J* = 8.3 Hz, 2H), 7.57 (d, *J* = 8.0 Hz, 1H), 7.44 – 7.37 (m, 1H), 7.07 (m, 3H), 6.28 (t, *J* = 5.5 Hz, 1H), 6.07 (s, 3H), 5.72 (s, 2H), 3.39 (m, 2H), 2.89 – 2.80 (m, 2H), 1.81-1.72 (m, 2H), 1.58 – 1.50 (m, 2H), 1.46 – 1.31 (m, 4H), 0.91 (t, *J* = 7.4 Hz, 6H). <sup>13</sup>C NMR (126 MHz, CDCl<sub>3</sub>) δ 166.8, 154.4, 151.0, 143.3, 138.6, 134.9, 134.2, 128.1, 127.6, 126.5, 126.0, 125.7, 122.8, 119.7, 114.7, 48.7, 39.9, 31.8,

29.9, 27.2, 22.6, 20.2, 13.8. HRMS  $m/z$ : calculated for  $C_{26}H_{32}N_5O^+$   $[M + H]^+$  430.2601, found 430.2609.

**4.1.16. 4-((4-amino-2-butyl-1*H*-imidazo[4,5-*c*]quinolin-1-yl)methyl)-*N*-octylbenzamide (19):** Compound **19** was synthesized similarly as described for compound **18**.  $^1H$  NMR (500 MHz,  $CDCl_3$ )  $\delta$  7.79 (dd,  $J = 8.4, 0.8$  Hz, 1H), 7.71 (d,  $J = 8.4$  Hz, 2H), 7.60 (dd,  $J = 8.3, 0.9$  Hz, 1H), 7.42 (ddd,  $J = 8.4, 7.1, 1.3$  Hz, 1H), 7.09 (m, 3H), 6.14 (t,  $J = 5.5$  Hz, 1H), 5.90 (s, 2H), 5.74 (s, 2H), 3.40 (m, 2H), 2.88 – 2.83 (m, 2H), 1.78 (m, 2H), 1.60 – 1.52 (m, 2H), 1.47 – 1.38 (m, 2H), 1.34 – 1.23 (m, 10H), 0.92 (t,  $J = 7.4$  Hz, 3H), 0.86 (t,  $J = 7.0$  Hz, 3H).  $^{13}C$  NMR (126 MHz,  $CDCl_3$ )  $\delta$  166.8, 154.2, 151.1, 143.8, 138.7, 135.0, 134.1, 128.1, 127.5, 126.7, 126.4, 125.8, 122.7, 119.7, 114.9, 48.8, 40.3, 31.9, 30.0, 29.7, 29.4, 29.3, 27.3, 27.1, 22.7, 22.6, 14.2, 13.9. HRMS  $m/z$ : calculated for  $C_{30}H_{40}N_5O^+$   $[M + H]^+$  486.3227, found 486.3225.

**4.1.17. 4-((4-amino-2-butyl-1*H*-imidazo[4,5-*c*]quinolin-1-yl)methyl)-*N*-isobutylbenzamide (20):** Compound **20** was synthesized similarly as described for compound **18**.  $^1H$  NMR (500 MHz,  $CDCl_3$ )  $\delta$  7.78 (d,  $J = 8.3$  Hz, 1H), 7.72 (d,  $J = 8.2$  Hz, 2H), 7.59 (d,  $J = 8.1$  Hz, 1H), 7.41 (t,  $J = 7.6$  Hz, 1H), 7.12 – 7.04 (m, 3H), 6.25 (t,  $J = 5.6$  Hz, 1H), 6.09 (s, 2H), 5.73 (s, 2H), 3.23 (t,  $J = 6.4$  Hz, 2H), 2.89 – 2.82 (m, 2H), 1.90 – 1.81 (m, 1H), 1.81 – 1.73 (m, 2H), 1.47 – 1.38 (m, 2H), 0.95 – 0.89 (m, 9H).  $^{13}C$  NMR (126 MHz,  $CDCl_3$ )  $\delta$  166.8, 154.2, 151.0, 143.3, 138.6, 134.9, 134.0, 127.9, 127.5, 126.5, 126.0, 125.7, 122.6, 119.6, 114.7, 48.6, 47.4, 29.9, 28.6, 27.1, 22.5, 20.1, 13.8. HRMS  $m/z$ : calculated for  $C_{26}H_{32}N_5O^+$   $[M + H]^+$  430.2601, found 430.2609.

**4.1.18. 4-((4-amino-2-butyl-1*H*-imidazo[4,5-*c*]quinolin-1-yl)methyl)-*N*-(2-hydroxy-2-methylpropyl)benzamide (21):** Compound **21** was synthesized similarly as described for compound **18**.  $^1H$  NMR (500 MHz,  $DMSO-d_6$ )  $\delta$  8.18 (t,  $J = 6.2$  Hz, 1H), 7.80 (d,  $J = 8.4$  Hz, 2H), 7.75 (dd,  $J = 8.3, 0.9$  Hz, 1H), 7.58 (dd,  $J = 8.3, 1.0$  Hz, 1H), 7.33 (ddd,  $J = 8.3, 7.0, 1.3$

Hz, 1H), 7.11 (d,  $J = 8.4$  Hz, 2H), 7.03 (ddd,  $J = 8.2, 7.1, 1.2$  Hz, 1H), 6.62 (s, 2H), 5.93 (s, 2H), 4.50 (s, 1H), 3.21 (d,  $J = 6.1$  Hz, 2H), 2.92 (t, 2H), 1.75 – 1.67 (m, 2H), 1.42 – 1.34 (m, 2H), 1.06 (s, 6H), 0.87 (t,  $J = 7.4$  Hz, 3H).  $^{13}\text{C}$  NMR (126 MHz, DMSO- $d_6$ )  $\delta$  166.3, 153.7, 151.6, 144.5, 139.7, 134.0, 132.9, 128.0, 126.4, 125.9, 125.4, 121.0, 120.0, 114.4, 69.8, 50.2, 47.9, 29.6, 27.4, 26.2, 21.2, 13.7. HRMS  $m/z$ : calculated for  $\text{C}_{26}\text{H}_{32}\text{N}_5\text{O}_2^+$   $[\text{M} + \text{H}]^+$  446.2551, found 446.2552.

**4.1.19. 4-((4-amino-2-butyl-1H-imidazo[4,5-c]quinolin-1-yl)methyl)-N-(2-hydroxyethyl)benzamide (22):** Compound **22** was synthesized similarly as described for compound **18**.  $^1\text{H}$  NMR (500 MHz, DMSO- $d_6$ )  $\delta$  8.42 (t,  $J = 5.6$  Hz, 1H), 7.80 (d,  $J = 8.3$  Hz, 2H), 7.75 (d,  $J = 8.1$  Hz, 1H), 7.61 (d,  $J = 8.0$  Hz, 1H), 7.37 (t,  $J = 7.7$  Hz, 1H), 7.10 (d,  $J = 8.3$  Hz, 2H), 7.07 (t,  $J = 7.7$  Hz, 1H), 7.01 (s, 2H), 5.94 (s, 2H), 4.73 (s, 1H), 3.30 – 3.24 (m, 2H), 2.95 – 2.89 (m, 2H), 1.73 – 1.65 (m, 2H), 1.41 – 1.32 (m, 2H), 0.85 (t,  $J = 7.4$  Hz, 3H).  $^{13}\text{C}$  NMR (126 MHz, DMSO- $d_6$ )  $\delta$  165.9, 154.3, 151.2, 139.6, 133.9, 133.4, 127.9, 127.0, 126.2, 125.4, 124.7, 121.6, 120.3, 114.1, 59.7, 48.0, 42.2, 29.6, 26.2, 21.8, 13.7. HRMS  $m/z$ : calculated for  $\text{C}_{24}\text{H}_{28}\text{N}_5\text{O}_2^+$   $[\text{M} + \text{H}]^+$  418.2238, found 418.2236.

**4.1.20. (4-((4-amino-2-butyl-1H-imidazo[4,5-c]quinolin-1-yl)methyl)phenyl)methanol (23):** To a solution of compound **11** (100 mg, 0.26 mmol) in dry THF (5 mL) was added  $\text{LiAlH}_4$  (8 mg, 0.26 mmol) in inert condition and stirred the reaction mixture for 10h at room temperature. Quench the  $\text{LiAlH}_4$  using 10% NaOH solution and decant the solvent. The solvent was removed under vacuum and the residue was purified using flash column chromatography (6% MeOH/dichloromethane) to obtain the desired product **23** (55 mg, 58%) as off-white solid.  $^1\text{H}$  NMR (500 MHz, DMSO- $d_6$ )  $\delta$  7.80 – 7.76 (m,  $J = 8.2, 0.8$  Hz, 1H), 7.57 (dd,  $J = 8.3, 1.0$  Hz, 1H), 7.33 (ddd,  $J = 8.3, 7.1, 1.2$  Hz, 1H), 7.26 (d,  $J = 8.2$  Hz, 2H), 7.06 – 7.01 (m, 1H), 6.98 (d,  $J = 8.1$  Hz, 2H), 6.56 (s, 2H), 5.84 (s, 2H), 5.12 (t,  $J = 5.7$  Hz, 1H), 4.43 (d,  $J = 5.3$  Hz, 2H), 2.93 – 2.87 (m, 2H), 1.75 – 1.67 (m, 2H), 1.42 – 1.34 (m, 2H),

0.87 (t,  $J = 7.4$  Hz, 3H).  $^{13}\text{C}$  NMR (126 MHz,  $\text{DMSO-}d_6$ )  $\delta$  153.6, 151.6, 144.6, 141.8, 134.9, 132.9, 127.0, 126.4, 126.3, 126.0, 125.2, 120.9, 120.1, 114.5, 62.5, 47.9, 29.5, 26.2, 21.8, 13.7. HRMS  $m/z$ : calculated for  $\text{C}_{22}\text{H}_{25}\text{N}_4\text{O}^+$   $[\text{M} + \text{H}]^+$  361.2023, found 361.2029.

## 4.2. TLR7 and TLR8 Reporter Cell Assays

Human embryonic kidney cells (HEK293) stably co-transfected with either human TLR7 gene (human TLR7-expressing HEK293 cells) or human TLR8 gene (human TLR8-expressing HEK293 cells) and an inducible SEAP (secreted embryonic alkaline phosphatase) reporter gene and mouse Raw-Blue cells with an inducible SEAP (secreted embryonic alkaline phosphatase) reporter gene were acquired from InvivoGen, USA. HEK293-blue and Raw-blue cells were cultured in DMEM supplemented with 10% (v/v) heat-inactivated fetal bovine serum, penicillin streptomycin 10,000 U/mL (Gibco) and Normocin 100  $\mu\text{g/mL}$  (InvivoGen). Cells were seeded at a density of approximately 40,000 cells/well in a volume of 180  $\mu\text{L}$ /well in a flat-bottom 96-well culture plate (Greiner-One). BBIQ, Imiquimod and Resiquimod (Sigma-Aldrich) were diluted in saline and added to culture plate containing relevant cells to the total volume of 200  $\mu\text{L}$ . The levels of SEAP were determined with QUANTI-Blue™ Solution (InvivoGen).

## 4.3 Molecular Modelling Studies

The three-dimensional structures of hTLR7 and hTLR8 were obtained from Protein Data Bank (PDB ID-TLR7: 5GMG, TLR8: 6WML). The docking study started with the definition of the binding site with the size and location of the binding site visualized in UCSF Chimera. All compound structures were drawn using Chems sketch. Binding mode and interaction of hTLR7 and hTLR8 with each of the compounds were performed using Autodock 4.2 software. This created a population of possible conformations and orientations for the ligands at the binding site. All calculations for protein-ligand docking were done using the

Lamarckian genetic algorithm (LGA) method. The docking site on the protein target was defined by establishing a grid box with the dimensions of X: -11.344 , Y: -29.041, Z: -16.746 for hTLR7 and X: 110.659, Y: 19.73, Z: 43.13 for hTLR8 with a grid spacing of 0.375. The best binding pose was chosen based on the lowest docking energy. Ten runs with Autodock were performed for each compound and for each run the best pose was saved. The interactions of all the docked complexes, including hydrogen bonds and bond lengths, were analyzed using UCSF Chimera and Ligplot+.

#### **4.4 Animal studies**

The study was carried out in accordance with the Australian Code of Practice for the Care and Use of Animals for Scientific Purposes (2013). The protocol was approved by the Animal Welfare Committee of Flinders University. All efforts were made to minimize animal suffering. Mice were housed in cages provisioned with water and standard food and monitored daily for health and condition. After final breeding all the mice were humanely euthanised. Spike protein (Q13 to P1209) of SARS-CoV-2 (Wuhan-Hu-1) reference sequence (GenBank accession: NC\_045512.2) was expressed in insect cells using recombinant baculovirus expression system (Vaccine 39, 2021, 5940–5953). The sequence of Sp was confirmed by mass spectroscopy, SDS-PAGE gel and Western blotting. Endotoxin was measured using a PyroGene Endotoxin Detection System (Cat. No. 50-658U, LONZA, Walkersville, MD, U.S.A.). Female, 6-8 weeks old C57BL/6 (BL6) mice were supplied by the College of Medicine and Public Health Animal Facility of Flinders University of South Australia. Mice were intramuscularly (i.m.) immunised with 0.5 µg of recombinant SARS-CoV-2 Spike (Sp) antigen alone or mixed with 10µg TLR7/8 agonist (0.1µg dose was used for compound 26 due to its toxicity) or 50µg Alhydrogel (Croda, Denmark) in the thigh muscle at weeks 0 and 2. Blood samples were collected by cheek vein bleeding at 2 weeks after each immunization. Sera were separated by centrifugation and stored at -20°C until use.



#### **4.5 Spike-specific antibody ELISA**

Spike-specific antibodies were determined by ELISA as previously described (Vaccine 39, 2021, 5940–5953). Briefly, a flat bottom 96-well ELISA plate (Greiner Bio-One) was coated with 1µg/ml of Sp in 100µl 0.1M carbonate buffer, pH 9.6 overnight at 4°C. Wells were blocked with 200µl of blocking buffer (0.2% Casein in 50mM Tris-HCl, pH 8.0 containing 1mM EDTA and 0.05% Tween-20) for 1 h at RT then 100µl of serum diluted in blocking buffer was added and incubated for 2h at RT. After washing, biotin-conjugated anti-mouse IgG (Sigma-Aldrich), IgG1, IgG2b, IgG2c, IgG3 and IgM (All from Abcam) mixed with HRP-conjugated streptavidin (BD Pharmingen, used at were added and incubated for 1 h at RT. After final wash, plates were incubated with 100µl of TMB substrate (KPL, Sera care) for 10 min and then the reaction was stopped by addition of 100µl of 1M phosphoric acid (Sigma-Aldrich), the optical density was measured at 450nm (OD<sub>450nm</sub>) using VersaMax ELISA microplate and analyzed using SoftMax Pro Software. Average OD<sub>450nm</sub> values obtained from negative control wells were subtracted.

#### **4.6 Statistical analysis**

All statistical analyses were performed using GraphPad Prism version 9.4.1 for Windows (GraphPad Software, La Jolla, CA, USA). The differences of antibody levels were evaluated by the Mann-Whitney test and other difference between groups were evaluated by two-tailed Student's t-test and  $p < 0.05$  was considered to represent a significant difference.

#### **Acknowledgements**

The project was also supported by funding from National Institute of Allergy and Infectious Diseases of the National Institutes of Health under Contracts HHS-N272201400053C and HHS-N272200800039C. The content is solely the responsibility of the authors and does not

necessarily represent the official views of the National Institutes of Health. This work was also supported by Australian Government Global Connections Fund Bridging Grant 511803900. DBS and NP are thankful to MHRD's Scheme for Promotion of Academic and Research Collaboration (SPARC/2018-2019/P385/SL) program of Govt. of India which aims to facilitate academic and research collaborations between Panjab University, Chandigarh and Flinders University, Adelaide, South Australia. DBS is thankful to Science and Engineering Research Board (SERB), New Delhi for the Core Research Grant (CRG/2021/005467), Department of Science & Technology & Renewable Energy, Chandigarh Administration, Paryavaran Bhawan, Chandigarh for Short Term Research Project and Indian Council of Medical Research, New Delhi for the ad-hoc research project. MTP is thankful to DST for the award of Women Scientist Scheme-A [SR/WOS-A/CS-132/2016 (G)].

## References

1. Akira, S.; Takeda, K.; Kaisho, T. Toll-like receptors: critical proteins linking innate and acquired immunity. *Nat. Immunol.* **2001**, *2*, 675-680.
2. Pasare, C.; Medzhitov, R. Toll-like receptors: linking innate and adaptive immunity. *Microbes Infect.* **2004**, *6*, 1382-1387.
3. Kaur, A.; Kaushik, D.; Piplani, S.; Mehta, S. K.; Petrovsky, N.; Salunke, D. B. TLR2 Agonistic Small Molecules: Detailed Structure–Activity Relationship, Applications, and Future Prospects *J. Med. Chem.* **2021**, *64*, 233–278.
4. Hood, J. D.; Warshakoon, H. J.; Kimbrell, M. R.; Shukla, N. M.; Malladi, S. S.; Wang, X.; David, S. A. Immunoprofiling toll-like receptor ligands: Comparison of

- immunostimulatory and proinflammatory profiles in ex vivo human blood models. *Hum. Vaccin* **2010**, *6*, 322-335.
5. Shukla, N. M.; Malladi, S. S.; Mutz, C. A.; Balakrishna, R.; David, S. A. Structure-activity relationships in human toll-like receptor 7-active imidazoquinoline analogues. *J. Med. Chem.* **2010**, *53*, 4450-4465.
  6. Gorden, K. B.; Gorski, K. S.; Gibson, S. J.; Kedl, R. M.; Kieper, W. C.; Qiu, X.; Tomai, M. A.; Alkan, S. S.; Vasilakos, J. P. Synthetic TLR agonists reveal functional differences between human TLR7 and TLR8. *J. Immunol.* **2005**, *174*, 1259-1268.
  7. Patinote, C.; Karroum, N. B.; Moarbess, G.; Cirnat, N.; Kassab, I.; Bonnet, P. A.; Deleuze-Masquéfa, C. Agonist and antagonist ligands of toll-like receptors 7 and 8: Ingenious tools for therapeutic purposes. *Eur. J. Med. Chem.* **2020**, *193*, 112238.
  8. Miller, R. L.; Gerster, J. F.; Owens, M. L.; Slade, H. B.; Tomai, M. A. Imiquimod applied topically: a novel immune response modifier and new class of drug. *Int. J. Immunopharmacol.* **1999**, *21*, 1-14.
  9. Isobe, Y.; Kurimoto, A.; Tobe, M.; Hashimoto, K.; Nakamura, T.; Norimura, K.; Ogita, H.; Takaku, H. Synthesis and biological evaluation of novel 9-substituted-8-hydroxyadenine derivatives as potent interferon inducers. *J. Med. Chem.* **2006**, *49*, 2088-2095.
  10. Koga-Yamakawa, E.; Dovedi, S. J.; Murata, M.; Matsui, H.; Leishman, A. J.; Bell, J.; Ferguson, D.; Heaton, S. P.; Oki, T.; Tomizawa, H.; Bahl, A.; Takaku, H.; Wilkinson, R. W.; Harada, H. Intratracheal and oral administration of SM-276001: a selective TLR7 agonist, leads to antitumor efficacy in primary and metastatic models of cancer. *Int. J. Cancer* **2013**, *132*, 580-590.

11. Anwar, M. A.; Shah, M.; Kim, J.; Choi, S. Recent clinical trends in Toll-like receptor targeting therapeutics. *Med. Res. Rev.* **2019**, *39*, 1053-1090.
12. Biggadike, K.; Ahmed, M.; Ball, D. I.; Coe, D. M.; Dalmas Wilk, D. A.; Edwards, C. D.; Gibbon, B. H.; Hardy, C. J.; Hermitage, S. A.; Hessey, J. O.; Hillegas, A. E.; Hughes, S. C.; Lazarides, L.; Lewell, X. Q.; Lucas, A.; Mallett, D. N.; Price, M. A.; Priest, F. M.; Quint, D. J.; Shah, P.; Sitaram, A.; Smith, S. A.; Stocker, R.; Trivedi, N. A.; Tsitoura, D. C.; Weller, V. Discovery of 6-Amino-2-[[[(1S)-1-methylbutyl]oxy]-9-[5-(1-piperidinyl)pentyl]-7,9-dihydro-8H-purin-8-one (GSK2245035), a Highly Potent and Selective Intranasal Toll-Like Receptor 7 Agonist for the Treatment of Asthma. *J. Med. Chem.* **2016**, *59*, 1711-1726.
13. Roethle, P. A.; McFadden, R. M.; Yang, H.; Hrvatin, P.; Hui, H.; Graupe, M.; Gallagher, B.; Chao, J.; Hesselgesser, J.; Duatschek, P.; Zheng, J.; Lu, B.; Tumas, D. B.; Perry, J.; Halcomb, R. L. Identification and optimization of pteridinone Toll-like receptor 7 (TLR7) agonists for the oral treatment of viral hepatitis. *J. Med. Chem.* **2013**, *56*, 7324-7333.
14. Kaushik, D.; Dhingra, S.; Patil, M. T.; Piplani, S.; Khanna, V.; Honda-Okubo, Y.; Li, L.; Fung, J.; Sakala, I. G.; Salunke, D. B.; Petrovsky, N. BBIQ, a pure TLR7 agonist, is an effective influenza vaccine adjuvant. *Hum. Vaccin. Immunother* **2020**, *16*, 1989-1996.
15. Saroa, R.; Kaushik, D.; Bagai, U.; Kaur, S.; Salunke, D. B. Efficacy of TLR7 agonistic imidazoquinoline as immunochemotherapeutic agent against P. Berghei ANKA infected rodent host. *Bioorg. Med. Chem. Lett.* **2019**, *29*, 1099-1105.
16. Ganneru, B.; Jogdand, H.; Dharam, V. K.; Molugu, N. R.; Prasad, S. D.; Vellimudu, S.; Ella, K. M.; Ravikrishnan, R.; Awasthi, A.; Jose, J.; Rao, P.; Kumar, D.; Ella, R.; Abraham, P.; Yadav, P.; Sapkal, G. N.; Shete, A.; Desphande, G. R.; Mohandas, S.;

- Basu, A.; Gupta, N.; Bharagava, B.; Vadrevu, K. M. Evaluation of Safety and Immunogenicity of an Adjuvanted, TH-1 Skewed, Whole Virion Inactivated SARS-CoV-2 Vaccine - BBV152. *bioRxiv* **2020**, 2020.09.09.285445.
17. Kaushik, D.; Kaur, A.; Petrovsky, N.; Salunke, D. B. Structural evolution of toll-like receptor 7/8 agonists from imidazoquinolines to imidazoles. *RSC Med. Chem.* **2021**, *12*, 1065-1120.
18. Shukla, N. M.; Mutz, C. A.; Ukani, R.; Warshakoon, H. J.; Moore, D. S.; David, S. A. Syntheses of fluorescent imidazoquinoline conjugates as probes of Toll-like receptor 7. *Bioorg. Med. Chem. Lett.* **2010**, *20*, 6384-6.
19. Shukla, N. M.; Kimbrell, M. R.; Malladi, S. S.; David, S. A. Regioisomerism-dependent TLR7 agonism and antagonism in an imidazoquinoline. *Bioorg. Med. Chem. Lett.* **2009**, *19*, 2211-4.
20. Shi, C.; Xiong, Z.; Chittepu, P.; Aldrich, C. C.; Ohlfest, J. R.; Ferguson, D. M. Discovery of Imidazoquinolines with Toll-Like Receptor 7/8 Independent Cytokine Induction. *ACS Med. Chem. Lett.* **2012**, *3*, 501-504.